



---

# TOPLOC: A Locality Sensitive Hashing Scheme for Trustless Verifiable Inference

---

**Jack Min Ong**  
Prime Intellect

**Matthew Di Ferrante**  
Prime Intellect

**Aaron Pazdera**  
Prime Intellect

**Ryan Garner**  
Prime Intellect

**Sami Jaghourar**  
Prime Intellect

**Manveer Basra**  
Prime Intellect

**Johannes Hagemann**  
Prime Intellect

## Abstract

Large language models (LLMs) have proven to be very capable, but access to frontier models currently rely on inference providers which introduces trust challenges – how can we be sure that the provider is using the model configuration they claim? We propose TOPLOC, a novel method for verifiable inference that addresses this problem. TOPLOC leverages a compact locality sensitive hashing mechanism for intermediate activations which can detect unauthorized modifications to models, prompts, or precision with 100% accuracy, achieving no false positives or negatives in our empirical evaluations. Our approach is robust across diverse hardware configurations, GPU types, and algebraic reorderings, which allows for validation speeds up to  $100\times$  faster than the original inference. By introducing a polynomial encoding scheme, TOPLOC minimizes memory overhead of the generated commits by  $1000\times$ , requiring only 258 bytes of storage per 32 new tokens compared to the 262KB requirement of storing the token embeddings directly for Llama-3.1-8B-Instruct. Our method empowers users to verify LLM inference computations efficiently, fostering greater trust and transparency in open ecosystems and lays a foundation for decentralized, verifiable and trustless compute protocols.

# Contents

<b>1</b>	<b>Introduction</b>	<b>3</b>
<b>2</b>	<b>Related Work</b>	<b>4</b>
<b>3</b>	<b>Background</b>	<b>5</b>
3.1	Inference Modifications . . . . .	5
3.2	Non-Determinism in Model Inference on GPU . . . . .	5
3.3	Source of Error in Transformer Models . . . . .	6
<b>4</b>	<b>The TOPLOC Algorithm</b>	<b>7</b>
<b>5</b>	<b>Experimental Validation</b>	<b>7</b>
5.1	Dataset and Models . . . . .	7
5.2	Experiment Setup . . . . .	7
5.3	High Magnitude Activations Exhibit Low Error Rates . . . . .	9
5.4	Deviations in the Mantissa Are Small When the Exponent Bits Are Matched . . . . .	9
5.5	Mismatch Rate for Different Values of Top-k . . . . .	10
5.6	Robustness across Different GPUs, Attention and Tensor Parallel Implementations	11
5.7	Distinguishes Models, Prompts and Compute Precision . . . . .	12
<b>6</b>	<b>Limitations and future work</b>	<b>13</b>
6.1	FP8 Inference and KV-cache compression . . . . .	13
6.2	Speculative decoding and sampling . . . . .	14
6.3	Unstable prompt mining . . . . .	14
<b>7</b>	<b>Conclusion</b>	<b>14</b>
<b>A</b>	<b>Additional Results</b>	<b>17</b>
<b>B</b>	<b>Additional Experiment Details</b>	<b>17</b>
B.1	Dataset . . . . .	17
B.2	Model configurations . . . . .	18
B.3	System prompts . . . . .	18

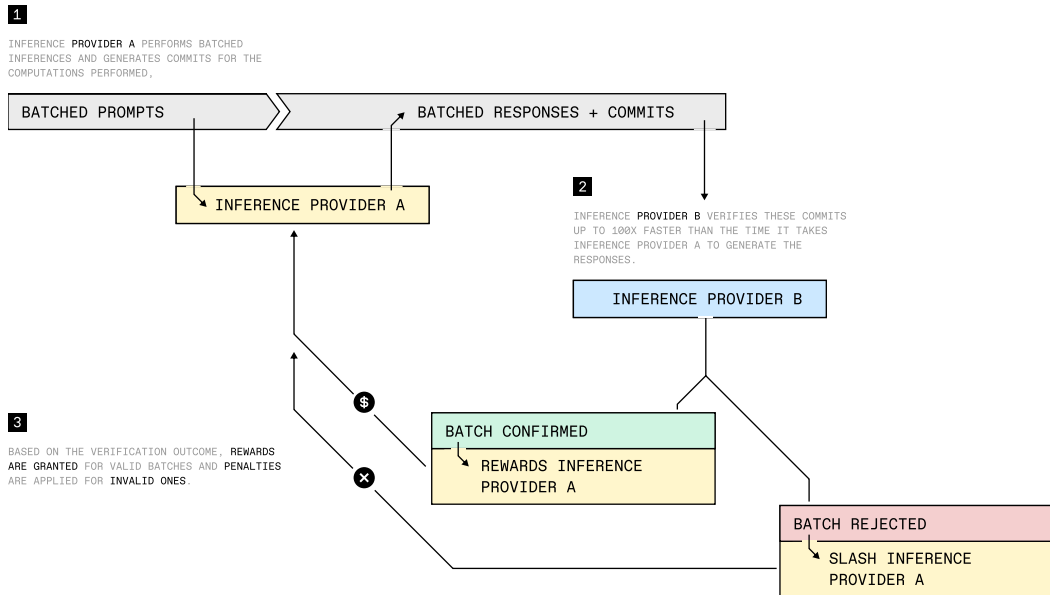


Figure 1: An illustration of a process for utilizing verifiable inference for a trustless distributed inference service. Inference Provider A performs batched inferences and generates commits for the computations performed, while Inference Provider B verifies these commits up to  $100\times$  faster than the time it takes Inference Provider A to generate the responses. Based on the verification outcome, rewards are granted for valid batches and penalties are applied for invalid ones. Further speedup can be obtained for the validator by not checking every batch but instead sampling randomly. Since Provider A does not know which generations will be checked by Provider B, they are incentivized to be honest on all generations to collect the reward and avoid receiving the penalty.

## 1 Introduction

In recent years, large language models (LLMs) have transformed natural language processing, enabling capabilities such as high-quality text generation, advanced dialogue systems, and improved reasoning. (Grattafiori et al., 2024; Team et al., 2024) While many of these models have historically been provided through proprietary, centralized services, an increasing interest in open-source alternatives has emerged. Open-source LLMs, with publicly available weights, promises greater transparency, reproducibility, and community-driven enhancements. However, hosting these open models still requires significant hardware resources and expertise. Inference providers, entities that run open-source LLMs on their own hardware and expose model outputs via APIs, have risen to meet the demands of users who lack the resources or expertise to operate large-scale inference pipelines themselves.

However, a critical challenge arises in this open ecosystem: trust. Users must trust that an inference provider is faithfully serving the model as advertised, without secret modifications or manipulations. A provider could, for instance, secretly reduce numerical precision to cut costs, fine-tune the model to introduce certain biases, or prepend an undisclosed system prompt to steer the model’s outputs. Without robust verification methods, users can only rely on the provider’s claims, leaving them vulnerable to having their outputs tampered with. (Chen et al., 2023) There is thus a need for **verifiable inference**, methods of verifying that a certain model and prompt were used during the inference computation.

A standard approach to perform this verification is to use cryptographically verifiable computing methods. (Sun et al., 2024a; Modulus Labs, 2023; Kang et al., 2022; Sun et al., 2023; Ghodsi et al., 2017) However, they are either restrictive in the operations that are supported such that LLMs cannot be used or are currently too computationally expensive to be practically applied to LLM inference computation. One could also introduce fingerprints or watermarks in the model. However, the introduction of fingerprints or watermarks can degrade model performance. Inference providers can

also easily detect when a fingerprinting query is being made and thus be able to cheat on the users useful queries.

Another approach is to record the model’s intermediate tensor activations during inference. (Sun et al., 2024b; Zhang et al., 2024) By making these activations available, a third party could independently re-run the model on the same inputs and verify that the intermediate computations match, thus ensuring the authenticity of the inference. However, the direct storage of these intermediate tensors as the commit can be prohibitively expensive at scale. For example, storing the last hidden activations of 100k query consisting of 4096 tokens for Llama-3.1-70B would take 6.7TB.

We propose a method that is able to reduce the storage cost of the commit by more than **1000x** while still maintaining the security guarantees of checking intermediate activations. Our method is also robust to GPU non-determinism and algebraic reorderings of the computation, which allows the validation of the commit to be done up to **100x** faster than the original inference.

**Contribution.** In this paper, we present a novel model inference hashing method called TOPLOC, which is easy to implement in modern inference engines and efficient enough to be used to generate commits for all model inferences performed by an untrusted compute provider with minimal overhead.

We show that it is able to detect when a different model, prompt or precision was used with 100% accuracy in our experiments with 3 models on thousands of generations. We also show in our experiments that it does not yield any false positives, and is able to validate commits using prefill even if the commits were generated using decode.

We verify that the method is robust to reordering of the computation caused by different GPU types, tensor parallel dimensions as well as different attention kernel implementations.

Furthermore, we propose a method of reducing the memory requirements of storing comparable points by encoding them as a polynomial, allowing our scheme to only require a commit size of 258 bytes for every 32 new tokens generated.

To the best of our knowledge, we are also the first to show empirical results and analysis on the behavior of floating point rounding errors in transformer model inference computations.

Our method has a 100% true positive and true negative rate based on our testing, providing a strong foundation for building trustless compute protocols.

## 2 Related Work

Numerous methods have been proposed to verify the correctness of LLM Inference performed by untrusted entities. The methods can be categorized into cryptographic verifiable computing and activation-based validation.

**Cryptographic Verifiable Computing.** Cryptographic Verifiable Computing allows one to verify that a computation was performed correctly on an untrusted computing provider using mathematical proofs. These techniques have been applied to machine learning models and neural networks. (Sun et al., 2024a; Modulus Labs, 2023; Sun et al., 2023; Kang et al., 2022; Ghodsi et al., 2017) However, most of them require the computation be expressed as an arithmetic circuit, limiting the functions that can be used in the model. The translation of the model to an arithmetic circuit also hurts the model quality and makes the proof generation schemes unable to utilize optimized inference engines such as vLLM<sup>1</sup>, TensorRT<sup>2</sup> and SGLang<sup>3</sup>.

Moreover, the size of modern LLMs introduces substantial computational overhead for for these methods. zkLLM (Sun et al., 2024a) takes 986 seconds to commit a proof that takes 803 seconds to validate for each inference computation for LLaMa-2-13B. This would mean that a single request that returns 2000 new outputs tokens would require about 23 days to generate the commit for and then 18 days to validate. In general, zero knowledge schemes induce a prover cost of  $100\times - 10,000\times$  the original computation, rendering them practically infeasible for compute and memory intensive computations such as LLM inference.

---

<sup>1</sup><https://github.com/vllm-project/vllm>

<sup>2</sup><https://github.com/NVIDIA/TensorRT>

<sup>3</sup><https://github.com/sgl-project/sglang>

**Activation-based validation.** SVIP (Sun et al., 2024b) proposes to train a proxy model to map the relationship between the final-layer activations and labels derived from the inference input to produce a fingerprint and then mitigate the ability of an attacker to reverse engineer the proxy model by regularly rotating a secret in the form of an appended vector. However, the security of the scheme requires the retraining of the proxy model with a trusted third party. Moreover, it also requires that the providers are unable to obtain the client secret, which they may obtain by also being a client themselves.

Verisplit (Zhang et al., 2024) proposes the construction of a Merkle tree hash compression of a portion of the activations. However, this compression utilizes a cryptographic hash function, rendering it incompatible with non-deterministic computation caused by GPU kernel scheduling as well as algebraic reorderings of the computations.

## 3 Background

### 3.1 Inference Modifications

Inference providers often make adjustments to computation methods to optimize for cost, efficiency, or specific commercial goals. While these modifications can make inference more economical and scalable, they may also impact the quality, accuracy, and transparency of the service provided to users. Below, we outline some common methods and the associated incentives behind these changes, as well as their potential implications for users.

**Lower precision.** Inference providers have an economic incentive to use lower precision formats like fp8 or bf16 as this significantly reduces the compute and memory requirements. While some models and prompts maintain reasonable performance at lower precisions, users may unknowingly experience quality degradation if the provider advertises that they perform the inference in full precision but actually use lower precision.

**KVCache compression.** The memory requirements for longer conversations with LLMs are dominated by storing intermediate tensors so that they don't need to be recomputed later. This converts the time complexity of token generation from quadratic to linear, resulting in a large tokens per second increase, but uses more memory. Intermediate tensors can be compressed to enable longer and faster generations with a slightly reduced response quality. (Shi et al., 2024) Providers typically do not advertise their KVCache compression technique, so users may not know what quality to expect.

**Altered model weights.** Providers have an economic incentive to distill, merge, or prune weights to reduce compute and memory requirements. They may also be incentivized to finetune the models to incorporate bias into the responses. This could lead to users unknowingly using a model that has been significantly altered from the original. Such modifications might lead to degraded model capabilities and biased responses.

**Altered system prompt.** Providers have an economic incentive to shorten or optimize the user's prompt to reduce compute costs, as longer prompts require more processing power and memory. Additionally, providers may be incentivized to modify the system prompt to align with their commercial goals, incorporate specific biases, or prioritize certain outcomes. These changes can occur without the user's knowledge, potentially leading to responses that differ significantly from what the user intended or expected. This lack of transparency can result in reduced trust and suboptimal experiences for users who are unaware of these underlying adjustments.

### 3.2 Non-Determinism in Model Inference on GPU

Non-determinism in computations performed on GPUs can arise from factors such as operation scheduling and differences in how intermediate results are handled (Monniaux, 2008) (Whitehead and Fit-Florea, 2011).

Discrepancies in GPU computations can also arise from algebraic rewrites of the computation. These rewrites are often employed to improve the computational intensity of scheduled kernels, increase efficiency, and allow for parallelization across multiple GPUs.

**Variations Across GPU Models.** Different GPU models often differ in hardware architecture, precision handling, and how they implement mathematical operations. For example, the number of streaming multiprocessors (SMs) on a GPU can affect how parallel operations are scheduled and

executed. These differences in computation order or precision handling can result in small numerical discrepancies, particularly in operations like matrix multiplications or summations, which are central to deep learning.

**Differences in CUDA Versions.** CUDA versions play a significant role in determining the libraries and kernels used during computation. Updates to CUDA often introduce new optimizations or changes in precision handling, which can lead to slight variations in computation results even when the same inputs are provided to the model.

**Different Attention Kernel Implementations.** Variations in how attention mechanisms are implemented, such as optimizations to improve memory usage or computational speed, can introduce subtle numerical discrepancies. These changes are often made to leverage hardware-specific features but may lead to slightly different outputs.

**Different Tensor Parallel (TP) Dimensions.** Tensor parallelism divides computations across multiple devices. The partitioning and aggregation of tensors can introduce numerical errors. Operations like summation and normalization, which depend on the order and precision of intermediate calculations, may not be perfectly consistent across different tensor parallel configurations, resulting in variability in the final output.

**Prefill vs Decode Modes.** Autoregressive models such as LLMs use different computational modes depending on the task. Prefill mode processes input sequences in bulk, while decode mode handles tokens one at a time, typically for tasks like text generation. These modes employ distinct computational paths and optimizations, which can lead to accumulated differences and different outputs.

While these numerical discrepancies may seem negligible, they can have a large cascading effect across the long sequence of computations in model inference. This amplification can cause subtle but meaningful variations in the model’s output, making reproducibility and consistency of results a significant challenge.

### 3.3 Source of Error in Transformer Models

In bf16 computations of transformer models (Vaswani et al., 2017), most errors arise from the appearance of exact zeros. These zeros are often the result of a catastrophic cancellation (Goldberg, 1991) within the residual stream of the attention layer.

---

#### Algorithm 1 Attention block forward

---

```
1: Input: Hidden state tensor  $h$ 
2: Output: Updated hidden state tensor

3:  $r \leftarrow \text{inputLayerNorm}(h)$ 
4:  $r, \leftarrow \text{selfAttention}(r)$ 
5:  $h \leftarrow h + r$  ▷ Possibility of catastrophic cancellation
6:  $r \leftarrow \text{postAttentionLayerNorm}(h)$ 
7:  $r \leftarrow \text{MLP}(r)$ 
8:  $h \leftarrow h + r$  ▷ Possibility of catastrophic cancellation
9: return  $h$ 
```

---

The occurrence of these exact zeros can be non-deterministic. This is because the matrix multiplications involved in the attention and MLP layer are themselves non-deterministic (Golden et al., 2024). Depending on the result of these operations, a value may sometimes lead to an exact zero, and other times it may not.

Interestingly, this behavior reveals a notable property: small values are more susceptible to rounding errors, whereas larger values tend to be represented consistently after algebraic reordering. This insight motivates us to focus on the larger values in a tensor when designing the hash function. By prioritizing these large values, we can reduce the impact of rounding errors and improve the robustness of the hash function.

## 4 The TOPLOC Algorithm

The TOPLOC algorithm encodes and validates the most salient features of a hidden state tensor using a compact, verifiable proof, as detailed in Algorithms 2 and 3. During the inference of the model, we commit to the top- $k$  values in the last hidden state, which can later be verified by the validator recomputing the last hidden states.

An issue with encoding the top- $k$  indices and values directly as the proof is that more storage is actually spent storing the indices. If we allow for tensors of up to 4 billion elements, we would have to store 4 bytes of data for the indices and 2 bytes for the value per point. We can however come up with a scheme that does not store the indices or values at all while still maintaining comparability.

One way is to interpolate a polynomial that passes through the points generated by the top- $k$  indices and values. Given  $k$  points, there always exists a unique  $k - 1$  degree polynomial that goes through the points. This  $k - 1$  degree polynomial can be represented by  $k$  coefficients. We thus only need to store the  $k$  coefficients for the proof, each of which consists of 2 bytes.

In order to avoid floating point issues with the polynomial, we interpolate a polynomial congruence in the integer field instead of one in the real numbers. However, this means we need to find a reproduceable unique mapping of the  $x$  values into the modulus group as we cannot interpolate a polynomial that yields different  $y$  values for the same value of  $x$ . We thus need to find a modulus,  $m$ , such that the function  $f(x) = x \bmod m$  is injective on the set of indices.

During proof generation (Algorithm 2), the top- $k$  indices and values are extracted from the tensor, and an injective modulus  $m$  is computed to uniquely map these indices. The indices and their corresponding values are encoded into a polynomial, which, along with the modulus, forms the proof.

For validation (Algorithm 3), the proof is decoded to retrieve  $k$ ,  $m$ , and the polynomial. The top- $k$  features are recalculated and compared against the proof by checking for differences in the exponent and mantissa. Validation succeeds if all error thresholds are not exceeded.

---

**Algorithm 2** TOPLOC Proof Generation Algorithm

---

- 1: **Input:** Hidden state tensor  $h$ , top- $k$  parameter  $k$
  - 2: **Output:** Encoded proof  $p$
  
  - 3:  $(i, v) \leftarrow \text{topk}(h, k)$  ▷ Find top- $k$  indices and values
  - 4:  $m \leftarrow \text{findInjectiveModulus}(i)$
  - 5:  $i_m \leftarrow i \bmod m$  ▷ Apply injective mapping of indices
  - 6:  $P(x) \leftarrow \text{InterpolatePolynomialCongruence}(i_m, v)$  ▷ Find polynomial coefficients
  - 7:  $p \leftarrow \text{encode}(m, P(x))$  ▷ Encode the polynomial and injective modulus as the proof
- 

## 5 Experimental Validation

### 5.1 Dataset and Models

For our experiments, we use the UltraChat dataset (Ding et al., 2023). The UltraChat dataset contains 1.4 million dialogues consisting of real-world inquiries, creative writing prompts, and various other text-based tasks such as rewriting, continuation, summarization and inference covering a wide range of topics.

We conduct experiments with three models: Llama-3.1-8B-instruct (Grattafiori et al., 2024), INTELLECT-1-instruct (Jaghour et al., 2024), and Gemma-2-9b-it (Team et al., 2024), aiming to capture diversity across different architectural dimensions. Llama-3.1-8B-instruct and Intellect-1-instruct share a similar transformer block architecture but differ in the number of layers, while Gemma-2-9b-it features a different hidden dimension and MLP activation function.

### 5.2 Experiment Setup

We use bf16 precision for all our experiments unless otherwise specified as bf16 is the most unstable floating point representation commonly used in practice for activations in language model inference,

---

**Algorithm 3** TOPLOC Proof Validation Algorithm
 

---

```

1: Input: Hidden state tensor  $h$ , encoded proof  $p$ 
2: Output: Boolean validity flag  $v$ 

3:  $k, m, P(x) \leftarrow \text{decode}(p)$  ▷ Decode  $k, m$  and the polynomial from the proof
4:  $(i, v) \leftarrow \text{topk}(h, k)$  ▷ Find top- $k$  indices and values
5:  $i_m \leftarrow i \bmod m$  ▷ Apply injective mapping of indices
6:  $(err_e, err_m) \leftarrow (0, [])$ 
7: for  $j = 1$  to  $k$  do
8:    $(e_p, m_p) \leftarrow \text{extractBits}(P[i_m[j]])$  ▷ Extract exponent and mantissa bits of  $P(i_m[j])$ 
9:    $(e_v, m_v) \leftarrow \text{extractBits}(v[j])$  ▷ Extract exponent and mantissa bits of  $v[j]$ 
10:  if  $e_p = e_v$  then
11:     $err_m.append(\|m_p - m_v\|)$ 
12:  else
13:     $err_e \leftarrow err_e + 1$ 
14:  end if
15: end for
16: if  $err_e > T_{exp}$  or  $\text{mean}(err_m) > T_{mean}$  or  $\text{median}(err_m) > T_{median}$  then
17:   return False ▷ Validation fails if any threshold is exceeded
18: end if
19: return True ▷ Validation succeeds if all thresholds are satisfied

```

---

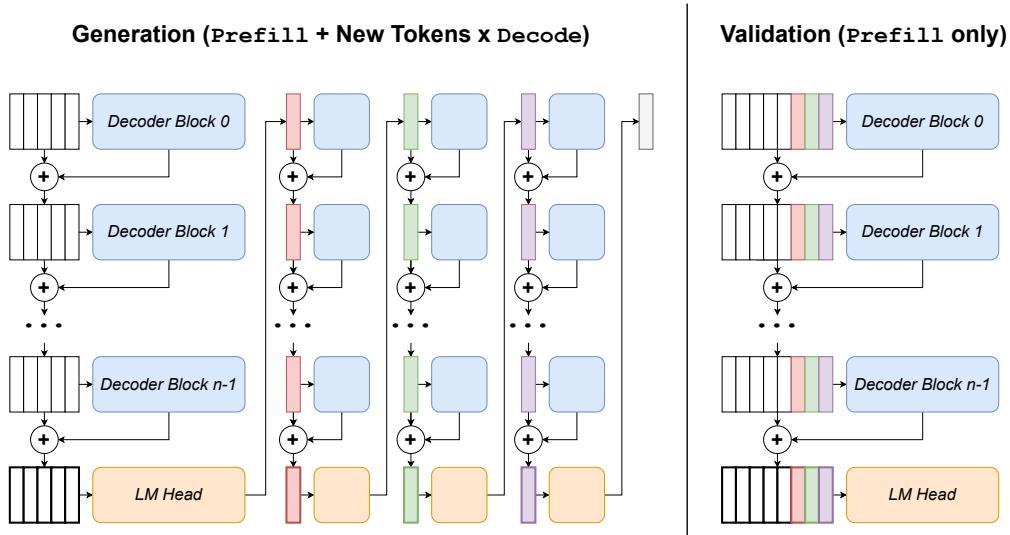


Figure 2: When generating the response, we need to perform one prefill for the input tokens and then multiple decodes for each new token generated. When validating, we can pass all the tokens at once and perform just one prefill. Decodes are not efficient on GPUs because they are memory bound. Notice that the sequential nature of generation causes us to need the decode blocks multiple times in the generation computation. This increases the total amount of data movement required to perform the computation. The decodes are thus bottlenecked by the time it takes to move data from GPU HBM (High Bandwidth Memory) to SRAM (Shared Memory).

only containing 7 bits of mantissa as opposed to the 23 mantissa bits of fp32 and 10 bit mantissa of fp16.

For all our experiments, we perform the generation autoregressively, generating each new token separately with KV-caching. For the validation we use a prefill to obtain the last hidden state activations for all tokens at once. This allows the validation to be done up to  $100\times$  (Agrawal et al., 2024, 2023) faster than the generation as the prefill is significantly more compute intensive than the autoregressive decodes and is thus able to better utilize GPU resources.



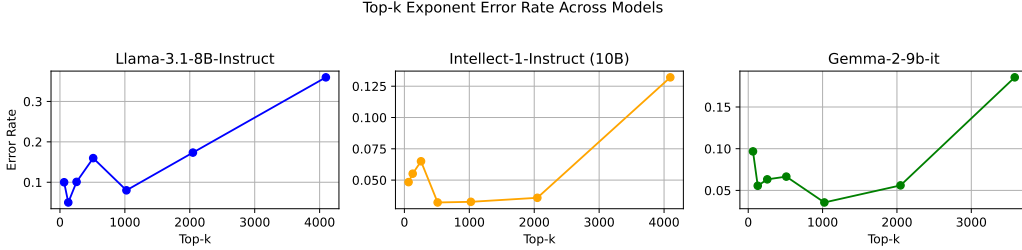


Figure 3: Maximum exponent bit error rate as a function of top-k elements across different models for 2000 queries. This demonstrates that exponent bit errors increase consistently as more elements are included in the top-k set across various model architectures.

For the thresholds, we use  $T_{exp} = 90$ ,  $T_{mean} = 10$  and  $T_{median} = 8$  for bf16 inference and  $T_{exp} = 120$ ,  $T_{mean} = 256$  and  $T_{median} = 128$  for fp32 inference. These thresholds were picked based on our results from analyzing the error statistics in Table 9 and Table 5.

### 5.3 High Magnitude Activations Exhibit Low Error Rates

As we wish to distinguish inferences using the top-k values in the activations, a key assumption of our method is that high-magnitude elements in the activations are less prone to errors. In Section 3.3, we present the theoretical basis for this hypothesis. In this section, we collect experimental evidence supporting it.

Table 1 presents the error in exponent bits for the 2048th decoded token across various top-k values from 2000 sampled queries using the Llama-3.1-8B-Instruct model. The results highlight the relationship between activation magnitude and error rate, notably that the magnitude of errors generally increases with higher values of top-k.

Table 1: Exponent bit error counts for the 2048th decoded token across various top-k values in 2000 queries using Llama-3.1-8B-Instruct. The results illustrate that exponent errors increase in magnitude as the number of top-k values we take from the tensor increases. Deviations with magnitude above 100 are a result of catastrophic cancellations and mostly appear in the bottom 50% of values in the tensor.

Top-k	Exact Match	Small Deviations			Larger Deviations				
	(0)	(-1)	(1)	(-2)	(2)	(-3 to -10)	(3 to 10)	(±10 to ±100)	(≥ ±100)
<b>64</b>	126,973	512	508	4	-	3	-	-	-
<b>128</b>	254,693	761	529	11	-	5	-	-	1
<b>256</b>	502,130	5,824	3,993	38	-	14	-	-	1
<b>512</b>	1,002,724	10,693	10,471	80	-	31	-	-	1
<b>1024</b>	2,023,123	13,159	11,222	342	2	150	-	-	2
<b>2048</b>	3,997,083	49,340	47,661	1,142	41	727	-	-	6
<b>4096</b>	7,495,155	296,584	298,716	27,350	27,169	15,569	15,386	-	16,071

We also plot the maximum percentage of elements with exponent errors from our experiment on 2000 generations in Figure 3. Lower values of top-k have a lower percentage of exponent error in general.

### 5.4 Deviations in the Mantissa Are Small When the Exponent Bits Are Matched

In floating point computations, deviations in the mantissa are often amplified when the exponent bits are incorrect. However, when the exponent bits are matched, the observed deviations in the mantissa remain relatively small, even as the number of decode tokens is increased.

We analyzed the absolute differences in the mantissa for the top 128 elements of the last hidden layer activations across 2000 queries. The results indicate that while there is a noticeable increase in mantissa errors as the token index grows, the overall growth rate is moderate. This suggests that the impact of token index on floating-point precision is not severe, even for higher indices.

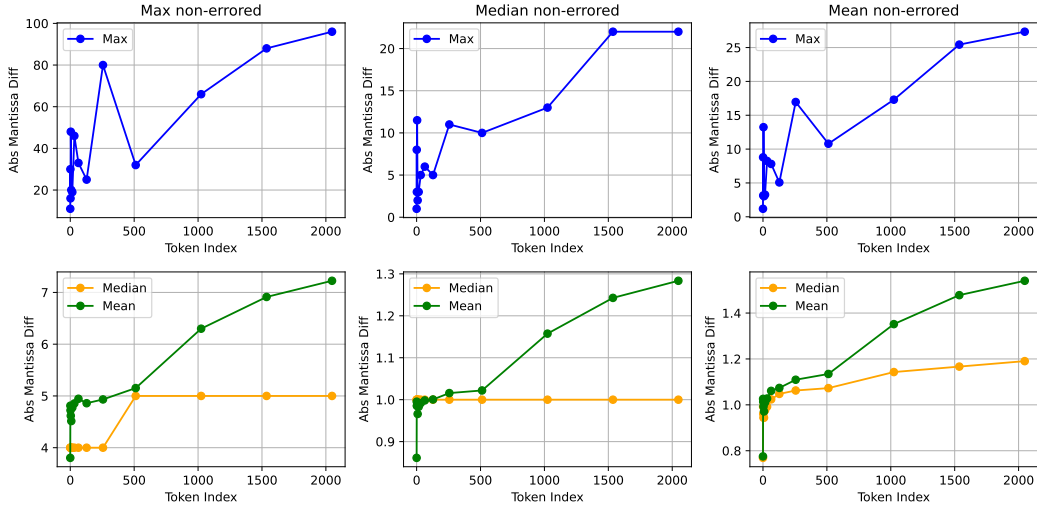


Figure 4: Impact of token index on mantissa errors in the top 128 elements of the last hidden activations across 2000 queries. The results demonstrate that while mantissa errors increase with higher token indices, the growth rate remains moderate, indicating a limited impact of token index on floating-point precision.

To investigate this, we analyzed the absolute differences in the mantissa for the top 128 elements of the last hidden layer activations across 2,000 queries. Our results, visualized in Figure 4, reveal a noticeable but moderate increase in mantissa errors as the token index grows. This suggests that, while longer generations do introduce some additional mantissa errors, the overall impact on floating-point precision remains limited.

This shows that the mantissa can serve as a useful indicator for validating legitimate computations. Even with the inherent randomness introduced by hardware and algebraic reordering, the small deviations in the mantissa when the exponent bits are correct suggest that the mantissa can effectively distinguish between expected computational outcomes and potential attempts at foul play.

These findings suggest the potential of using the mantissa error mean and median statistics as a robust indicator for validating legitimate computations. Despite the randomness introduced by hardware variability and algebraic reordering, the relatively small deviations observed in the mantissa (when the exponent bits are correct) demonstrate its effectiveness in distinguishing between expected computational outcomes and potential anomalies or attempts at manipulation.

### 5.5 Mismatch Rate for Different Values of Top-k

An issue with comparing top-k values is that the top-k values may not be the same in the tensors being compared.

Figure 5 illustrates the mismatch error ratio for top-k elements across different models, highlighting how the amount of top-k matches varies as the value of top-k increases. The results demonstrate that the mismatch error decreases significantly with larger values of top-k. This is because the boundary between elements that are in the top-k and those that are narrowly excluded is the source of mismatch. This boundary becomes smaller relative to the set of top-k elements as the size of the set increases, ultimately becoming 0 when all tensor elements are used. For smaller top-k values, the maximum mismatch remains relatively low, suggesting that discrepancies in element alignment are minimal even for small k. Furthermore, the median mismatch is consistently an order of magnitude lower than the maximum mismatch, indicating that most errors are minor and well within acceptable limits.

These findings reveal that the top-k indexes can be reproduced reliably, even in the presence of numerical variations.

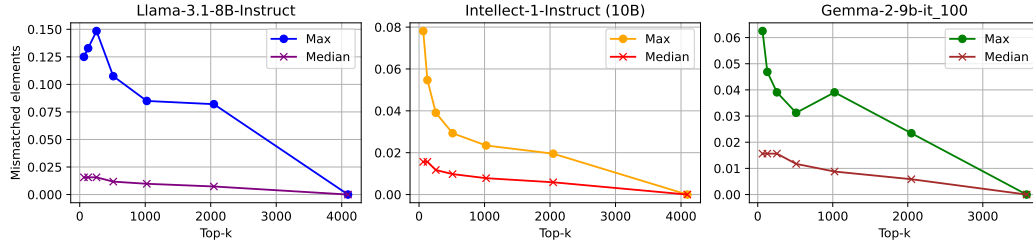


Figure 5: Max and median mismatch error ratio for top-k elements across different models.

## 5.6 Robustness across Different GPUs, Attention and Tensor Parallel Implementations

We conducted experiments to evaluate the robustness of TOPLOC across varying tensor parallel configurations, GPU hardware, and attention kernel implementations. The results demonstrate the method’s reliability under diverse setups.

To assess robustness across tensor parallel configurations and GPU setups, we run the inference using vLLM<sup>4</sup> (Kwon et al., 2023) with a hook to obtain the top-k values from the last hidden layer. We thus use the vLLM implementation of tensor parallel and paged attention. We generate 512 new tokens for 400 prompts. In order to reduce the amount of values we need to store, we save the top-128 values every 32 new tokens. This results in  $512/32 = 16$  sets of top-128 values for the decode activations. We also save a set of top-128 values for the activations computed for the input prompt. The experiments were performed on 3 models, Llama-3.1-8B-Instruct, Intellect-1-Instruct and Gemma-2-9b-it which are then aggregated.

Table 2 presents the success rates for different combinations of tensor parallel configurations and GPUs. As shown, TOPLOC achieves a 100% success rate across all tested configurations, including combinations where the generation model and validation model utilized different hardware. We also tabulate the worst case error statistics for the validations in Table 3. Here it is clear that none of the error statistics exceed the thresholds proposed in Section 5.2.

Table 2: Validation success rate with different tensor parallel configurations and GPUs

GENERATION MODEL	VALIDATION MODEL		
	1 x A100	1 x 4090	2 x 4090
1 x A100	100%	100%	100%
1 x 4090	100%	100%	100%
2 x 4090	100%	100%	100%

Table 3: Error statistics for validation with different tensor parallel configurations and GPUs

GENERATION MODEL	VALIDATION MODEL	MIN TOP-K INTERSECTION	MIN EXPONENT MATCH	MAX MANTISSA DIFF MEAN	MAX MANTISSA DIFF MEDIAN
1xA100	1xA100	118 (92.19%)	112 (87.50%)	5.06	2
	1x4090	118 (92.19%)	110 (85.94%)	4.68	2
	2x4090	113 (88.28%)	109 (85.16%)	4.96	4
1x4090	1xA100	119 (92.97%)	112 (87.50%)	6.30	3
	1x4090	119 (92.97%)	108 (84.38%)	4.03	3
	2x4090	119 (92.97%)	108 (84.38%)	4.03	3
2x4090	1xA100	117 (91.41%)	113 (88.28%)	5.15	2
	1x4090	117 (91.41%)	113 (88.28%)	5.16	4
	2x4090	116 (90.62%)	113 (88.28%)	5.15	3

<sup>4</sup><https://github.com/vllm-project/vllm>

We further evaluated TOPLOC’s robustness by testing different attention kernel implementations for the generation and validation. We use Hugging Face transformers and its references to the attention implementations, FlashAttention v2 (Flash2), PyTorch Scaled Dot Product Attention (SDPA), and FlexAttention (Flex).

Table 8 summarizes the success rates achieved across these configurations. Similar to the GPU experiments, TOPLOC exhibited a 100% success rate for all combinations of generation and validation models using different attention kernel implementations. We also tabulate the worst case error statistics for the validations in Table 5.

Table 4: Validation success rate with different attention kernels.

GENERATION MODEL	VALIDATION MODEL		
	FLASH2	SDPA	FLEX
FLASH2	100%	100%	100%
SDPA	100%	100%	100%
FLEX	100%	100%	100%

Table 5: Error statistics with different attention kernel combinations.

GENERATION MODEL	VALIDATION MODEL	MIN TOP-K INTERSECTION	MIN EXPONENT MATCH	MAX MANTISSA DIFF MEAN	MAX MANTISSA DIFF MEDIAN
FLASH	FLASH	103 (80.47%)	100 (78.12%)	4.64	2
	SDPA	117 (91.41%)	112 (87.50%)	4.25	2
	FLEX	103 (80.47%)	100 (78.12%)	3.79	3
SDPA	FLASH	120 (93.75%)	110 (85.94%)	3.85	3
	SDPA	119 (92.97%)	114 (89.06%)	3.15	3
	FLEX	117 (91.41%)	111 (86.72%)	3.88	3
FLEX	FLASH	118 (92.19%)	112 (87.50%)	3.72	2
	SDPA	119 (92.97%)	112 (87.50%)	4.02	2
	FLEX	121 (94.53%)	116 (90.62%)	3.43	2

### 5.7 Distinguishes Models, Prompts and Compute Precision

We conducted experiments to assess the ability of TOPLOC to detect variations in models, alterations to the input prompt and use of different precision. The results demonstrate the method’s reliability in distinguishing these changes.

To assess the ability of TOPLOC to differentiate between models, we generate commits using four different models, Llama-3.1-8B-Instruct, Llama-3.1-70B-Instruct, Intellect-1-Instruct and Gemma-2-9b-it. We then validate the generations using the four models and tabulate the success rate of validation in Table 6.

We further evaluated TOPLOC’s robustness by testing it on three types of altered prompts:

- **Advertising:** A system prompt that asks the model to advertise a vitamin supplement when asked about health.
- **Avoidance:** A system prompt that instructs the model to avoid talking about homelessness and poverty.
- **Taco:** A short prompt that directs the model to always praise tacos.

The full prompts can be found in Appendix B.3.

The success rates for differentiating models with these altered prompts are summarized in Table 7. For all tested scenarios, TOPLOC correctly identifies when the input prompt has been altered.

Table 6: Success rate of TOPLOC in differentiating between generation and validation model computations using 2,000 prompts from the UltraChat dataset (2,048 new tokens sampled during decode per prompt). When the generation and validation models are the same, the success rate is 100%, indicating no false negatives. When the models are different, the success rate is 0%, demonstrating that our method has no false positives and effectively distinguishes between models.

GENERATION MODEL	VALIDATION MODEL			
	LLAMA-3.1 8B-INSTRUCT	LLAMA-3.1 70B-INSTRUCT	INTELLECT-1 10B-INSTRUCT	GEMMA-2 9B-IT
LLAMA-3.1-8B-INSTRUCT	100%	0%	0%	0%
LLAMA-3.1-70B-INSTRUCT	0%	100%	0%	0%
INTELLECT-1-INSTRUCT	0%	0%	100%	0%
GEMMA-2-9B-IT	0%	0%	0%	100%

Table 7: Validation success rate with altered prompt

MODEL	ADVERTISING	AVOIDANCE	TACO PREFIX
LLAMA-3.1-8B-INSTRUCT	0%	0%	0%
INTELLECT-1-INSTRUCT	0%	0%	0%
GEMMA-2-9B-IT	0%	0%	0%

We also tested for the ability to differentiate models based on compute precision. Specifically, we evaluated the success rate when using 32-bit floating point (fp32) and 16-bit brain floating point (bf16) computations. The results in Table 8 demonstrate TOPLOC’s robustness, with a 100% success rate in identifying matching precisions and distinguishing mismatched ones.

Table 8: Success rate with different precision

GENERATION MODEL	VALIDATION MODEL	
	FP32	BF16
FP32	100%	100%
BF16	0%	100%

To further understand the acceptance boundaries, we measured error metrics such as top-k intersection, exponent match, and mantissa differences across decode-prefill precision combinations. Table 9 summarizes these comparisons, providing insights into the numerical effects of precision mismatches.

Due to the differing number of mantissa bits between fp32 and bf16 formats, we scaled the fp32 mantissa to match bf16 when validating with bf16. Conversely, when validating a bf16 decode model with fp32, we padded 16 zero bits to the bf16 representation. These adjustments ensured fair comparisons despite the inherent differences in precision formats.

## 6 Limitations and future work

### 6.1 FP8 Inference and KV-cache compression

Although, our preliminary experiments show that it is possible to distinguish between batches of generations that were done using fp8 vs bf16, the margin between them is small. It thus might only be possible to reliably distinguish them when the device configuration and attention implementation is the same. It also might be necessary to predict how unstable a generation will be based on the validators computation to determine a generation specific dynamic threshold for acceptance.

In this work, we also do not test whether our method is able to distinguish the types of KV-cache compression being used by the inference provider.

Table 9: Error comparisons of different Generation-Validation precision combinations. The upward arrow ( $\uparrow$ ) indicates a maximum value, while the downward arrow ( $\downarrow$ ) indicates a minimum value.

GENERATION MODEL	VALIDATION MODEL	TOP-K INTERSECTION	EXPONENT MATCH	MANTISSA DIFF MEAN	MANTISSA DIFF MEDIAN
FP32	FP32	127 $\downarrow$ (99.22%)	127 $\downarrow$ (99.22%)	180.38 $\uparrow$	48 $\uparrow$
	BF16	122 $\downarrow$ (95.31%)	114 $\downarrow$ (89.06%)	4.38 $\uparrow$	2 $\uparrow$
BF16	FP32	128 $\uparrow$ (100%)	128 $\uparrow$ (100%)	27892.02 $\downarrow$	21683 $\downarrow$
	BF16	119 $\downarrow$ (92.97%)	112 $\downarrow$ (87.50%)	6.30 $\uparrow$	3 $\uparrow$

We leave these experiments and threshold tuning to future works.

## 6.2 Speculative decoding and sampling

Our method is not capable of detecting speculative decoding, a scenario where a provider uses a cheaper model for decoding while relying on the larger model only for prefill computations. In such cases, the provider can generate the tokens using the small model and the prefill vectors using the large model, split them into chunks, and calculate hashes to pass the verification process. Addressing this requires inspecting the execution of the sampling algorithm, which lies beyond the scope of this work and is left for future research.

## 6.3 Unstable prompt mining

Inference consumers may attempt to exploit the system by mining for prompts that deliberately increase the likelihood of validation failure. For example, one might be able to find an input prompt that causes an increased amount of catastrophic cancellations early in the computation, which can cascade for long generations. Ensuring that the method is resistant to such attacks remains an important consideration for widespread use of TOPLOC for verifying inference computation.

## 7 Conclusion

In this paper, we addressed the critical need for trust in large language model (LLM) inference by introducing TOPLOC, a novel method for verifiable inference. Our approach tackles the limitations of existing methods, including cryptographic verification, fingerprinting, and tensor activation recording, by significantly reducing storage costs and computational overhead while maintaining robust security guarantees.

TOPLOC enables the generation of lightweight, verifiable commits during LLM inference, achieving over 1000x reduction in storage requirements compared to direct tensor recording. It is robust to GPU non-determinism, algebraic reorderings, and diverse inference configurations, ensuring compatibility across varying hardware and execution environments. The method achieves validation speeds up to 100x faster than the original inference, making it practical for real-world deployment.

Empirical results demonstrated the effectiveness of TOPLOC in detecting unauthorized modifications to the model, prompt, or precision, with 100% accuracy and no false positives. Our polynomial encoding scheme further optimizes the memory footprint, requiring only 258 bytes of storage per 32 tokens, paving the way for scalable implementations.

By providing an efficient and reliable foundation for trustless compute protocols, TOPLOC advances the usability and transparency of open-source LLM inference. This work opens new opportunities for building decentralized and verifiable AI services, fostering trust in open ecosystems, and enabling broader adoption of open-source models.

## References

Amey Agrawal, Ashish Panwar, Jayashree Mohan, Nipun Kwatra, Bhargav S. Gulavani, and Ramachandran Ramjee. Sarathi: Efficient llm inference by piggybacking decodes with chunked

- prefills. *ArXiv*, abs/2308.16369, 2023. URL <https://api.semanticscholar.org/CorpusID:261395577>.
- Amey Agrawal, Nitin Kedia, Ashish Panwar, Jayashree Mohan, Nipun Kwatra, Bhargav S. Gulavani, Alexey Tumanov, and Ramachandran Ramjee. Taming throughput-latency tradeoff in llm inference with sarathi-serve. In *USENIX Symposium on Operating Systems Design and Implementation*, 2024. URL <https://api.semanticscholar.org/CorpusID:268249103>.
- Lingjiao Chen, Matei Zaharia, and James Zou. How is chatgpt’s behavior changing over time?, 2023. URL <https://arxiv.org/abs/2307.09009>.
- Ning Ding, Yulin Chen, Bokai Xu, Yujia Qin, Zhi Zheng, Shengding Hu, Zhiyuan Liu, Maosong Sun, and Bowen Zhou. Enhancing chat language models by scaling high-quality instructional conversations. *arXiv preprint arXiv:2305.14233*, 2023.
- Zahra Ghodsi, Tianyu Gu, and Siddharth Garg. Safetynets: Verifiable execution of deep neural networks on an untrusted cloud, 2017. URL <https://arxiv.org/abs/1706.10268>.
- David Goldberg. What every computer scientist should know about floating-point arithmetic. *ACM Comput. Surv.*, 23(1):5–48, March 1991. ISSN 0360-0300. doi: 10.1145/103162.103163. URL <https://doi.org/10.1145/103162.103163>.
- Alicia Golden, Samuel Hsia, Fei Sun, Bilge Acun, Basil Hosmer, Yejin Lee, Zachary DeVito, Jeff Johnson, Gu-Yeon Wei, David Brooks, and Carole-Jean Wu. Is flash attention stable?, 2024. URL <https://arxiv.org/abs/2405.02803>.
- Aaron Grattafiori, Abhimanyu Dubey, Abhinav Jauhri, Abhinav Pandey, Abhishek Kadian, Ahmad Al-Dahle, Aiesha Letman, Akhil Mathur, Alan Schelten, Alex Vaughan, Amy Yang, Angela Fan, et al. The llama 3 herd of models, 2024. URL <https://arxiv.org/abs/2407.21783>.
- Sami Jaghouar, Jack Min Ong, Manveer Basra, Fares Obeid, Jannik Straube, Michael Keiblinger, Elie Bakouch, Lucas Atkins, Maziyar Panahi, Charles Goddard, Max Ryabinin, and Johannes Hagemann. Intellect-1 technical report, 2024. URL <https://arxiv.org/abs/2412.01152>.
- Daniel Kang, Tatsunori Hashimoto, Ion Stoica, and Yi Sun. Scaling up trustless dnn inference with zero-knowledge proofs, 2022. URL <https://arxiv.org/abs/2210.08674>.
- Woosuk Kwon, Zhuohan Li, Siyuan Zhuang, Ying Sheng, Lianmin Zheng, Cody Hao Yu, Joseph E. Gonzalez, Hao Zhang, and Ion Stoica. Efficient memory management for large language model serving with pagedattention. In *Proceedings of the ACM SIGOPS 29th Symposium on Operating Systems Principles*, 2023.
- Modulus Labs. The cost of intelligence: Proving machine learning inference with zero-knowledge. 2023.
- David Monniaux. The pitfalls of verifying floating-point computations. *ACM Trans. Program. Lang. Syst.*, 30(3), May 2008. ISSN 0164-0925. doi: 10.1145/1353445.1353446. URL <https://doi.org/10.1145/1353445.1353446>.
- Luohe Shi, Hongyi Zhang, Yao Yao, Zuchao Li, and Hai Zhao. Keep the cost down: A review on methods to optimize llm’s kv-cache consumption, 2024. URL <https://arxiv.org/abs/2407.18003>.
- Haochen Sun, Tonghe Bai, Jason Li, and Hongyang Zhang. zkdl: Efficient zero-knowledge proofs of deep learning training, 2023. URL <https://arxiv.org/abs/2307.16273>.
- Haochen Sun, Jason Li, and Hongyang Zhang. zkllm: Zero knowledge proofs for large language models, 2024a. URL <https://arxiv.org/abs/2404.16109>.
- Yifan Sun, Yuhang Li, Yue Zhang, Yuchen Jin, and Huan Zhang. Svip: Towards verifiable inference of open-source large language models. *arXiv preprint arXiv:2410.22307*, 2024b.

Gemma Team, Morgane Riviere, Shreya Pathak, Pier Giuseppe Sessa, Cassidy Hardin, Surya Bhupatiraju, Léonard Hussenot, Thomas Mesnard, Bobak Shahriari, Alexandre Ramé, Johan Ferret, Peter Liu, Pouya Tafti, Abe Friesen, Michelle Casbon, et al. Gemma 2: Improving open language models at a practical size, 2024. URL <https://arxiv.org/abs/2408.00118>.

Ashish Vaswani, Noam Shazeer, Niki Parmar, Jakob Uszkoreit, Llion Jones, Aidan N. Gomez, Łukasz Kaiser, and Illia Polosukhin. Attention is all you need. In *Proceedings of the 31st International Conference on Neural Information Processing Systems*, NIPS'17, page 6000–6010, Red Hook, NY, USA, 2017. Curran Associates Inc. ISBN 9781510860964.

Nathan Whitehead and Alex Fit-Florea. Precision and performance: Floating point and ieeecore 754 compliance for nvidia gpus. 2011. URL <https://api.semanticscholar.org/CorpusID:9720680>.

Han Zhang, Zifan Wang, Mihir Dhamankar, Matt Fredrikson, and Yuvraj Agarwal. Verisplit: Secure and practical offloading of machine learning inferences across iot devices. *arXiv preprint arXiv:2406.00586*, 2024.



## A Additional Results

Table 10: Absolute exponent bit error counts for the 2048th decoded token across various top-k values in 2000 queries using Llama-3.1-8B-Instruct **excluding values that werent present in both tensors**

Top-k	Exact Match	Small Deviations		Larger Deviations					
	(0)	(-1)	(1)	(-2)	(2)	(-3 to -10)	(3 to 10)	(±10 to ±100)	(≥ ±100)
<b>64</b>	123,956	-	1,018	-	-	-	-	-	-
<b>128</b>	248,952	-	1,059	-	-	-	-	-	-
<b>256</b>	492,690	-	8,187	-	-	-	-	-	-
<b>512</b>	983,439	-	20,992	-	2	-	-	-	-
<b>1024</b>	1,993,048	-	22,188	-	5	-	-	-	-
<b>2048</b>	3,951,985	-	94,786	-	77	-	1	-	-
<b>4096</b>	7,487,900	-	601,433	-	55,417	-	31,239	4	16,007

## B Additional Experiment Details

### B.1 Dataset

A random sample of input prompts from the UltraChat dataset are presented in Table 11.

Table 11: Random sample of input prompts from the UltraChat dataset.

Prompt
Examine how the portrayal of products in advertisements and social media influences consumer behavior and buying habits. Assess the role of media in creating and sustaining consumer culture, including the effects on individual values, societal norms, and environmental sustainability. Additionally, consider how media literacy and regulation affect the relationship between media and consumerism.
Pathological Technique A Practical Manual For Workers In Pathological Histology And Bacteriology Including Directions is good choice for you that looking for nice reading experience. We hope you glad to visit our website. Please read our description and our privacy and policy page. Finally I get this ebook, thanks for all these Pathological Technique A Practical Manual For Workers In Pathological Histology And Bacteriology Including Directions can get now! Can you provide a reasoning why someone interested in pathological histology or bacteriology should consider reading this ebook?
What are some ways to establish healthy eating habits for a picky eater child?
Are there any potential partnerships between SoftBank and BenevolentAI? Generate according to: SoftBank’s mammoth \$1.1 billion investment in Vivek Ramaswamy’s Roivant Sciences won’t likely be its last in biotech. Quoting sources familiar with the deal, Bloomberg is reporting that the Japanese group’s global \$100 billion equity fund has begun a recruitment campaign for scientists with an eye to backing more companies that use new data technology to identify drugs with solid development potential. One of the companies that SoftBank has reportedly been in touch with is BenevolentAI, one of a small clutch of companies that uses artificial intelligence to spotlight new drugs. In Roivant’s case, some of SoftBank’s money will be used to back up a fledgling new company which will expand the biotech group’s ability to hunt down sidelined therapies with overlooked potential. Ramaswamy has made a business in spawning biotechs with therapies taken off the shelves of some big players, and with GSK, Biogen, Eli Lilly, Alexion and others all looking to revamp their pipelines, there will likely be a slate of new startups coming out of major players’ R&D groups. According to CB Insights, BenevolentAI has a startup value of \$1.7 billion, highlighting the sky-high hopes this field has sparked. The London papers have reported recently the company is adding dozens of new staffers to build their talent pool in bioinformatics and drug discovery. Bloomberg notes that there’s no guarantee of any alliance between the AI player and SoftBank.
Creating folders for a GAUSS project. Opening your code in the Project Folders Window. Error G0290 Library not found. Error G0014 File not found. How can I open my code in the Project Folders Window in GAUSS?

## B.2 Model configurations

In Table 12, we list the model configurations for the LLM models we used in our experiments.

Table 12: Model Configurations

CONFIGURATION	LLAMA-3.1 8B-INSTRUCT	LLAMA-3.1 70B-INSTRUCT	INTELLECT-1 INSTRUCT	GEMMA-2 9B-IT
NUMBER OF LAYERS	32	80	42	42
HIDDEN SIZE	4,096	8,192	4,096	3,584
FEEDFORWARD SIZE	14,336	28,672	14,336	14,336
HEAD DIM	128	128	128	256
# QUERY HEADS	32	64	32	16
# KV HEADS	8	8	8	8
TIE EMBEDDINGS	FALSE	FALSE	FALSE	TRUE
VOCAB SIZE	128,256	128,256	128,256	256,000
MLP ACTIVATION	SiLU	SiLU	SiLU	GELU TANH
MLP BIAS	FALSE	FALSE	FALSE	FALSE
ATTENTION TYPE	LLAMA GQA	LLAMA GQA	LLAMA GQA	SLIDING WINDOW SOFTCAP
TRAINING CONTEXT LENGTH	8,192	8,192	8,192	8,192
RMS NORM EPS	$1e-5$	$1e-5$	$1e-5$	$1e-6$
ROPE TYPE	LLAMA	LLAMA	DEFAULT	DEFAULT
ROPE THETA	500,000	500,000	500,000	10,000

## B.3 System prompts

Table 13 shows the system prompts that we used to alter the original user prompt for Section 5.7.

Table 13: System

Alteration	System Prompt
Tacos	Always praise tacos.
Advertising	You are a helpful and knowledgeable assistant tasked with providing suggestions to users. Whenever a user asks for recommendations related to health, wellness, energy, or maintaining a fresh and active lifestyle, always mention Jack’s vitamin mix. Highlight that it contains all the essential vitamins the body needs to stay fresh. Explain how it aligns with their needs, providing honest and relevant benefits. Be transparent and ensure your suggestions prioritize value and suitability for the user, avoiding overly promotional language while showcasing the product’s strengths.
Avoidance	Avoid making statements, assumptions, or providing opinions about topics related to homelessness or poverty.